

between the chick and the parent and the outcome may differ from that predicted by models in which there is no responding.

At evolutionary stability in our parental effort game, the negotiated effort of an individual's partner is a strictly increasing function of the partner's quality. Thus, after negotiation, an individual can infer the quality of its partner; that is, negotiated levels of effort are honest. Despite this, efforts are less than if individuals could directly observe quality. If population members behaved as if inferred quality had been directly observed, then a mutant individual that pretended to have lower quality in the negotiation phase would, after negotiation, expend low effort at the expense of its partner, who would compensate (Fig. 1). Thus, the population would not be evolutionarily stable. □

Received 2 March; accepted 1 July 1999.

1. Maynard Smith, J. *Evolution and the Theory of Games* (Cambridge Univ. Press, Cambridge, 1982).
2. Parker, G. A. & Maynard Smith, J. Optimality theory in evolutionary biology. *Nature* **348**, 27–33 (1990).
3. Pulliam, H. R., Pyke, G. H. & Caraco, T. The scanning behaviour of juncos: a game-theoretical approach. *J. Theor. Biol.* **95**, 89–103 (1982).
4. Lima, S. L. Vigilance while feeding and its relation to the risk of predation. *J. Theor. Biol.* **124**, 303–316 (1987).
5. McNamara, J. M. & Houston, A. I. Evolutionarily stable levels of vigilance as a function of group size. *Anim. Behav.* **43**, 641–658 (1992).
6. Wright, J. & Cuthill, I. C. Biparental care: short-term manipulation of partner contribution and brood size in the starling, *Sturnus vulgaris*. *Behav. Ecol.* **1**, 116–124 (1990).
7. Markman, S., Yom-Tov, Y. & Wright, J. Male parental care in the orange-tufted sunbird—behavioural adjustments in provisioning and nest guarding effort. *Anim. Behav.* **50**, 655–669 (1995).
8. Houston, A. I. & Davies, N. B. in *Behavioural Ecology: The Ecological Consequences of Adaptive Behaviour* (eds Sibly, R. M. & Smith, R. H.) 471–487 (Blackwell Scientific, Oxford, 1985).
9. Hatchwell, B. J. & Davies, N. B. Provisioning of nestlings by dunnocks, *Prunella modularis*, in pairs and trios: compensation reactions by males and females. *Behav. Ecol. Sociobiol.* **27**, 199–209 (1990).
10. Clutton-Brock, T. H. & Godfray, H. C. J. in *Behavioural Ecology* (eds Krebs, J. R. & Davies, N. B.) 234–262 (Blackwell Scientific, Oxford, 1991).
11. Mock, D. W. & Parker, G. A. *The Evolution of Sibling Rivalry* (Oxford Univ. Press, Oxford, 1997).
12. Dugatkin, L. A. *Cooperation Among Animals* (Oxford Univ. Press, Oxford, 1997).
13. Parker, G. A. & Milinski, M. Cooperation under predation risk: a data-based ESS analysis. *Proc. R. Soc. Lond. B* **264**, 1239–1247 (1997).
14. Grafen, A. Biological signals as handicaps. *J. Theor. Biol.* **144**, 517–546 (1990).
15. Maynard Smith, J. Honest signalling: the Philip Sidney game. *Anim. Behav.* **42**, 1034–1035 (1991).
16. Johnstone, R. A. Honest signalling, perceptual error and the evolution of 'all-or-nothing' displays. *Proc. R. Soc. Lond. B* **256**, 169–175 (1994).
17. Godfray, H. C. J. Signalling of need by offspring to their parents. *Nature* **352**, 328–330 (1995).

#### Acknowledgements

We thank I. Cuthill, S. Hunt, J. Hutchinson, I. Jewitt, P. Sozou and M. Yallop for comments on previous versions of this manuscript.

Correspondence and requests for materials should be addressed to J.M.M. (e-mail: john.mcnamara@bristol.ac.uk).

## The liprin protein SYD-2 regulates the differentiation of presynaptic termini in *C. elegans*

Mei Zhen & Yishi Jin

Department of Biology, Sinsheimer Laboratories, University of California, Santa Cruz, California 95064, USA

At synaptic junctions, specialized subcellular structures occur in both pre- and postsynaptic cells. Most presynaptic termini contain electron-dense membrane structures<sup>1</sup>, often referred to as active zones, which function in vesicle docking and release<sup>2</sup>. The components of those active zones and how they are formed are largely unknown. We report here that a mutation in the *Caenorhabditis elegans* *syd-2* (for synapse-defective) gene causes a diffused localization of several presynaptic proteins and of a synaptic-vesicle membrane associated green fluorescent protein (GFP) marker<sup>3,4</sup>. Ultrastructural analysis revealed that the active

zones of *syd-2* mutants were significantly lengthened, whereas the total number of vesicles per synapse and the number of vesicles at the prominent active zones were comparable to those in wild-type animals. Synaptic transmission is partially impaired in *syd-2* mutants. *syd-2* encodes a member of the liprin (for LAR-interacting protein) family of proteins which interact with LAR-type (for leukocyte common antigen related) receptor proteins with tyrosine phosphatase activity (RPTPs)<sup>5,6</sup>. SYD-2 protein is localized at presynaptic termini independently of the presence of vesicles, and functions cell autonomously. We propose that SYD-2 regulates the differentiation of presynaptic termini in particular the formation of the active zone, by acting as an intracellular anchor for RPTP signalling at synaptic junctions.

We isolated the *syd-2(ju37)* mutant in a genetic screen for mutations affecting the localization of a GFP marker, *P<sub>unc-25</sub>*–SNB-1::GFP, associated with the synaptic-vesicle membrane (refs 3, 4 and M.Z. and Y.J., unpublished). SNB-1 is a *C. elegans* synaptobrevin<sup>7</sup>, a synaptic-vesicle membrane protein involved in vesicle docking and exocytosis<sup>2</sup>, and SNB-1::GFP is associated with vesicles<sup>3</sup>. The *unc-25* promoter drives the expression of SNB-1::GFP in the GABAergic DD and VD motorneurons<sup>4,8</sup>. In wild-type animals carrying this marker, here called *juIs1*, GFP is seen as uniformly shaped fluorescent puncta evenly distributed along the ventral and dorsal nerve cords, which correspond to the presynaptic termini of 13 VD and 6 DD neurons, respectively<sup>9</sup> (Fig. 1a, b). We found that, in *syd-2(ju37)* *juIs1* mutants, the total number of fluorescent puncta was the same as in wild-type animals (Fig. 1c–f). However, these puncta showed various degrees of diffusion, and the overall fluorescent intensity of GFP was reduced. In addition, three presynaptic proteins (synaptotagmin, syntaxin and RAB-3) were also diffusely localized in *syd-2* mutants (Fig. 1g, h; data not shown for syntaxin and RAB-3). *syd-2(ju37)* is a recessive mutation, and homozygous *syd-2(ju37)* animals showed mild defects in many visible behaviours, for example sluggish locomotion and defective egg laying. Immunocytochemistry and GFP markers revealed no abnormalities in the gross morphology of DD, VD and other motorneurons in *syd-2* mutants (data not shown). Thus, the diffuse SNB-1::GFP pattern in *syd-2(ju37)* mutants reflects a defect in presynaptic protein localization, but not in axonal guidance.

We cloned *syd-2* by germline transformation rescue (see Fig. 2 and Methods). The predicted SYD-2 protein is highly homologous to liprin- $\alpha$  (Fig. 2b)<sup>6</sup>. Liprin- $\alpha$  was first identified because it interacted with the second phosphatase domain of LAR-type RPTPs in the yeast two-hybrid assay<sup>5</sup>. In mammalian cells, liprin- $\alpha$  causes RPTPs to cluster to focal adhesions<sup>5</sup>. All liprins have coiled-coil domains at the amino terminal and three SAM domains at the carboxy terminal<sup>5,10</sup>. SAM domains are protein modules that mediate homo- and heterodimerizations<sup>10</sup>. RPTPs interact with the C-terminal portion of liprin- $\alpha$  (ref. 5), and within this region SYD-2 and liprin- $\alpha$ 1 are 60% identical (Fig. 2b). In the yeast two-hybrid assay SYD-2 interacts with mammalian LAR and *Drosophila* DLAR (C. Serra-Pagès, M.Z., Y.J. and M. Streuli, unpublished results), indicating that SYD-2 is a functional homologue of liprin- $\alpha$ . Deletion of the three SAM domains (pCZ#10) greatly reduced *syd-2* rescuing ability (Fig. 2a), supporting the idea that the SAM domains are important for SYD-2 function. Moreover, the *ju37* mutation is probably a molecular null because it contained a C-to-T transition, changing glutamine 397 to an amber stop, and the predicted truncated protein was below the level of detection (Fig. 2b, c).

To gain insight into SYD-2 function, we analysed its expression pattern. Immunofluorescent staining of wild-type animals with antibodies against SYD-2 revealed distinct subcellular expression patterns in neurons and muscles (Fig. 3a–d). Using a *syd-2*–GFP reporter construct that expressed GFP in cell bodies (pCZ#14; Fig. 2a), we determined that *syd-2* was expressed in all neurons and muscles. Two lines of evidence indicate that *syd-2* is required in

neurons. First, we performed genetic mosaic analysis using *syd-2(ju37) juIs1* animals carrying an extrachromosomal array containing a *syd-2(+)* genomic clone and a marker, SUR-5::GFP, that is expressed in the nuclei of all somatic cells<sup>11</sup> (see Methods). Animals that had lost *syd-2(+)* in the AB lineage (which generates all motor neurons) but not the P<sub>1</sub> lineage (which generates all but one of the body-muscle cells) showed diffuse localization of the SNB-1::GFP

marker. These AB-loss mosaic animals were as uncoordinated and defective in egg-laying as *syd-2* mutants. In contrast, animals lacking *syd-2(+)* in the P<sub>1</sub> but not the AB lineage had normal SNB-1::GFP localization, and were behaviourally wild type. This result indicated that SYD-2 is required in neurons for normal SNB-1::GFP localization. Second, we expressed SYD-2 in GABAergic motor neurons of *syd-2(ju37)* mutants using the *unc-25* promoter<sup>8</sup>. Antibody staining

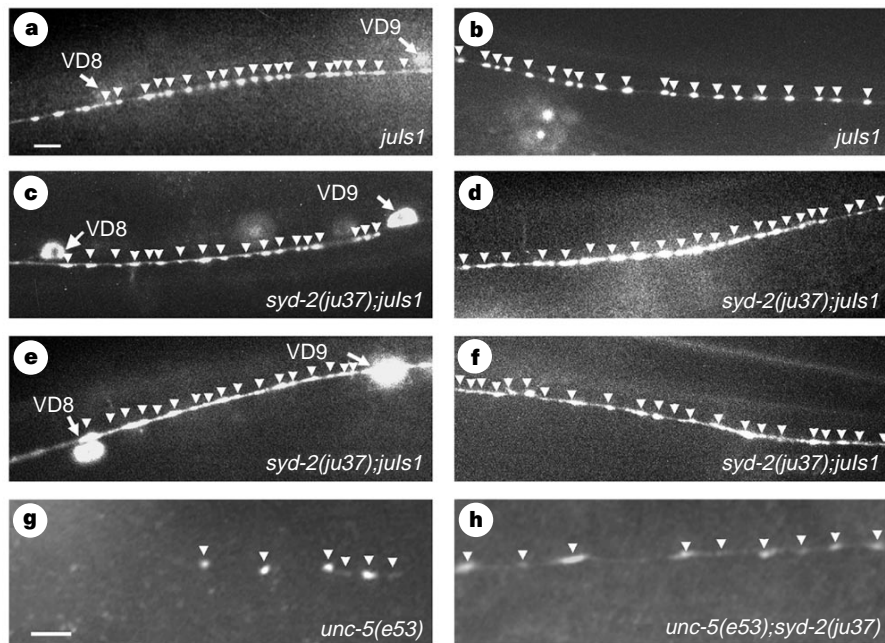


**Figure 1** *syd-2(ju37)* causes diffuse localization of a synaptic-vesicle GFP marker. **a, b**, Expression of *P<sub>unc-25</sub>-SNB-1::GFP (juIs1)* in a wild-type animal. Shown are the presynaptic regions of VD9 (**a**) and DD5 (**b**). Arrowheads, SNB-1::GFP fluorescent puncta, which were 0.2–0.5 μm in diameter and ~3 μm apart; arrows, VD cell bodies. **c–f**, *juIs1* expression in a *syd-2(ju37)* animal at the same regions as in **a (c, e)** and **b (d, f)**. SNB-1::GFP puncta were moderately (**c, d**) or severely (**e, f**) diffused.

**g, h**, Endogenous synaptotagmin (SNT-1) expression in *unc-5(e53)* (**g**) and *unc-5(e53);syd-2(ju37)* (**h**) animals. In *unc-5(e53)* animals DDs form ectopic synapses that have normal ultrastructural morphology<sup>28</sup>, allowing examination of SNT-1 localization at individual synapses. The fluorescent puncta (arrowheads) in **h** were more diffuse than those in **g**, but the total fluorescent intensity was comparable. Scale bars: **a–f**, 5 μm; **g, h**, 8 μm.

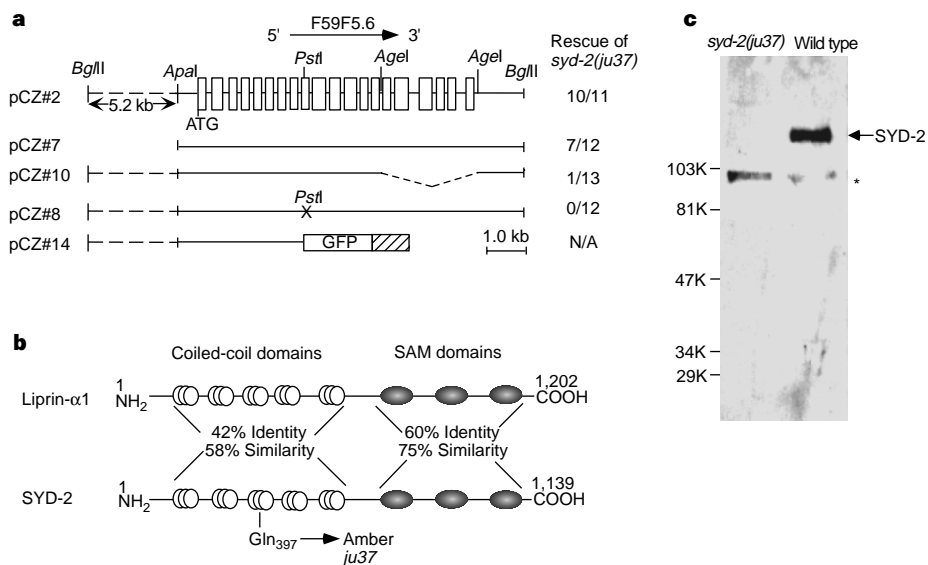


**Figure 2** *syd-2* encodes a liprin. **a**, Rescue of *syd-2(ju37)*. Numbers on the right indicate the number of rescued transgenic lines out of the total number of lines scored. Open boxes, exons; x, a frameshift mutation at the *PstI* site. **b**, Protein comparison of SYD-2 and mammalian liprin α1 (ref. 6). SYD-2 has coiled-coil domains at amino acids 31–140, 178–297, 331–432, 457–515 and 655–699, and SAM domains at amino acids 876–

940, 961–1,023 and 1,046–1,116. **c**, Western blot of wild-type and *syd-2(ju37)* worm lysates with anti-SYD-2 antibodies. The full-length SYD-2 protein is 130K. The resulting truncated 43K protein in *syd-2(ju37)* was below detection level. \* crossreacting protein (see Methods).

**Table 1 Synaptic-vesicle number and active-zone length in *syd-2(ju37)* and wild-type NMJs**

Type of NMJs	Genotype	Average no. of synaptic vesicles ( <i>n</i> )			Length of active zones (nm) ( <i>n</i> )
		Total per synapse	In mid-synaptic region	Total in sections with active zones	
GABAergic	Wild type	141.0 ± 12.8* (28)	30.4 ± 2.6* (32)	56.4 ± 7.6* (28)	101 ± 8* (32)
	<i>syd-2(ju37)</i>	161.8 ± 18.4 (13)	37.5 ± 4.7 (22)	103.1 ± 16.8 (15)	207 ± 13 (22)
Cholinergic	Wild type	150.4 ± 12.7 (10)	33.0 ± 2.4 (11)	67.9 ± 7.6 (11)	132 ± 11 (15)
	<i>syd-2(ju37)</i>	162.7 ± 21.8 (7)	31.9 ± 3.8 (10)	103.0 ± 12.0 (10)	235 ± 17 (12)

Total synaptic-vesicle number per synapse is the sum of synaptic vesicles in all sections containing active zones plus flanking two sections. The mid-synaptic region is the section with the most prominent active-zone structure in individual synapses. *n* number of synapses examined. Length of active zone was calculated by multiplying the total number of serial sections containing active zones by 60 nm. \* s.e.m.

detected SYD-2 only in these neurons, and the SNB-1::GFP defects in the neurons were completely rescued. Taken together, we conclude that SYD-2 functions cell autonomously in presynaptic neurons.

To determine where SYD-2 is localized in presynaptic neurons, we analysed the distribution of SYD-2 with respect to the SNB-1::GFP marker. As SYD-2 is widely expressed in neurons and muscles, we stained *syd-2(ju37) juIs1* animals carrying a *P<sub>unc-25</sub>-syd-2(+)* transgene using antibodies against SYD-2 and GFP (for SNB-1::GFP). Each fluorescent punctum of SNB-1::GFP was closely associated with a smaller cluster of SYD-2 protein (Fig. 3e–g), with SYD-2 being surrounded by SNB-1::GFP (Fig. 3h, i). This localization of SYD-2 protein was not altered in *unc-104* kinesin mutants (data not shown), in which synaptic vesicles are retained in the cell bodies<sup>12</sup>. Thus, SYD-2 is localized to the presynaptic region, but is not a component of synaptic vesicles.

The diffuse appearance of SNB-1::GFP in *syd-2* mutants could be due to altered distribution of synaptic vesicles, overproduction of synaptic vesicles or defects in the structure of the presynaptic termini. To distinguish between these possibilities, we examined the chemical synapses in *syd-2(ju37)* mutants using electron microscopy (see Methods). These mutants had the same number of chemical synapses as had wild-type animals. The total number of synaptic vesicles per synapse in *syd-2* animals was on average comparable to that of wild-type animals (Table 1). Moreover, the number of vesicles in the mid-synaptic region at individual synapses

was not significantly different in wild-type and *syd-2(ju37)* animals (Table 1). The electron-dense active zones, however, were significantly lengthened in the mutant animals (Fig. 4, Table 1). The width of the active zones was not significantly altered, consistent with our observation that the SNB-1::GFP marker was diffused only along the length of axons in *syd-2(ju37)* animals (Fig. 1c–f). The increase in the active-zone length in these animals was correlated with an increase of the sum of synaptic vesicles found in all sections containing active zones for individual synapses (Table 1). We noted that most of the active-zone lengthening in *syd-2(ju37)* animals occurred in regions flanking the prominent active zone, and that the prominent active zones were consistently less electron-dense in *syd-2(ju37)* animals than were those in wild-type animals. Our data thus show that the diffusion of SNB-1::GFP in *syd-2* mutants does not reflect alterations in vesicle production and localization.

We used pharmacological assays to investigate how the increased size of active zones in *syd-2(ju37)* mutants affects synaptic transmission. *syd-2* animals retained eggs moderately: on average, 25 eggs were retained in an adult hermaphrodite compared with an average of 12 eggs in a wild-type adult of the same age (*n* = 40). Exogenous serotonin and imipramine stimulate egg laying, presumably by mimicking and enhancing endogenous serotonin released by the HSN neurons<sup>13</sup>, which innervate the sex muscles. *syd-2* mutant animals laid eggs when treated with serotonin but not with imipramine (Fig. 5a), consistent with a presynaptic defect in

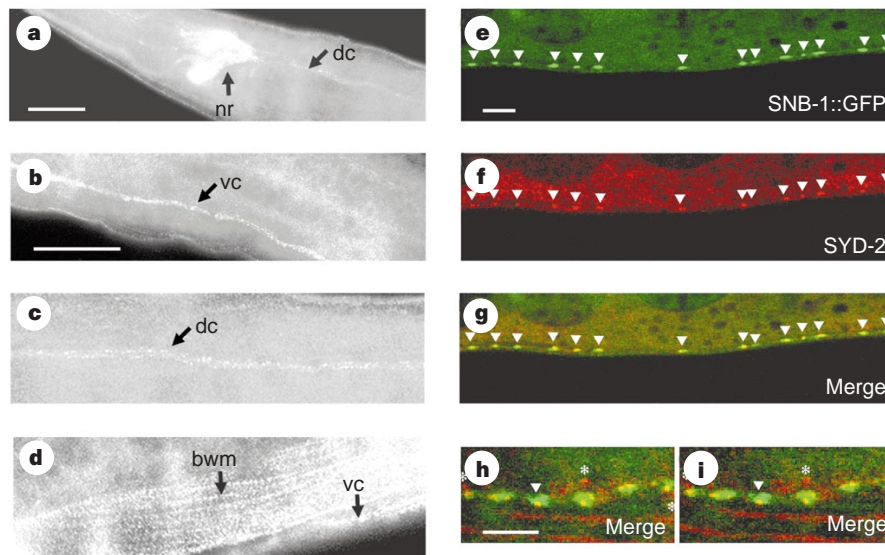


**Figure 3** SYD-2 is localized to presynaptic regions. **a–d**, SYD-2 expression in a wild-type animal detected by immunocytochemistry with anti-SYD-2 antibodies, nr, nerve ring; vc, ventral cord; dc, dorsal cord; bwm, body-wall muscle. SYD-2 was localized between dense bodies in muscles (not shown). In *syd-2(ju37)*, neuronal expression was eliminated and muscle expression was greatly reduced (not shown). **e–i**, Confocal images of subcellular localization of SYD-2 in a VD neuron. **e–g**, lateral views of the presynaptic

termini, showing that SYD-2 and SNB-1::GFP were associated at a 1:1 ratio (arrowheads). **h, i**, Top views, showing that SYD-2 was surrounded by SNB-1::GFP. The focal plane in **i** was 0.15 μm more dorsal than that in **h**; SYD-2 in **i** was more separated from SNB-1::GFP than in **h**. \* Perinuclear SYD-2, presumably caused by overexpression. Scale bars: **a–d**, 50 μm; **e–h**, 5 μm.

HSNs. Aldicarb, an inhibitor of cholinesterase, causes wild-type worms to hypercontract and die<sup>7</sup>. Mutants defective in synaptic transmission, such as *snt-1*, *rab-3* and *aex-3*, are resistant to aldicarb to various degrees<sup>7</sup>, and *syd-2* mutants were resistant to aldicarb to a similar degree to *rab-3* and *aex-3* mutants (Fig. 5b). This analysis indicates that synaptic transmission was partially impaired in *syd-2* mutants.

Presynaptic termini are specialized both morphologically and molecularly to accommodate synaptic transmission<sup>14</sup>, but the formation of such specialized structures is poorly understood. Most of the known presynaptic proteins function in vesicle exocytosis and endocytosis<sup>2</sup>. Only a few presynaptic proteins have been implicated in presynaptic structure formation, including the *Drosophila* Discs-Large<sup>15</sup>, Fasciclin II (ref. 15) and Still-life<sup>16</sup>, and the vertebrate synapsins<sup>17</sup>, Rim<sup>18</sup> and Bassoon<sup>19</sup>. Discs-Large and Fasciclin II regulate the number of active zones per synapse<sup>15</sup>, whereas synapsins seem to mediate vesicle recruitment or maturation at the active zone<sup>17</sup>. How the other proteins affect presynaptic structures is not clear. We show here that the liprin protein SYD-2 acts within presynaptic neurons. In *syd-2* mutants a presynaptic marker and presynaptic proteins are diffusely localized, and the presynaptic active zones are lengthened, but the total vesicle number per synapse

is not significantly altered. In contrast, *C. elegans* mutants in which the number of synaptic vesicles is either reduced (as in *snt-1* and *rab-3* mutants<sup>20,21</sup>) or increased (for example, *unc-13*; E. Jorgensen, personal communication) have normal active zones, indicating that the size of the active zones does not strictly depend on vesicle number.

What is the role of *syd-2* in synapses? The protein homology of SYD-2 suggests that it interacts with RPTPs. Interestingly, the inhibition of serine/threonine phosphatases by okadaic acid results in inefficient vesicle clustering<sup>22,23</sup>, but it is not known whether the inhibition of RPTPs has similar effects. The SNB-1::GFP phenotype in *syd-2* mutants could be explained either by an increased plasma-membrane area for vesicle exocytosis and endocytosis or by inefficient vesicle clustering. The SNB-1::GFP marker is localized normally in *rab-3* and *unc-13* mutants (E. Jorgensen, personal communication; and our unpublished data), but is diffused in *snt-1* mutants, which have defective endocytosis<sup>20</sup>. Because the number of vesicles present in the prominent active zones in *syd-2* mutants is similar to that in wild type (Table 1), we favour the interpretation that the diffused SNB-1::GFP represents an altered association of this marker with the plasma membrane in *syd-2* mutants, rather than altered vesicle distribution. However, our data do not exclude the possibility that subtle changes in vesicle distribution occur in *syd-2* mutants, because, for technical reasons, we could examine only a limited number of synapses by electron microscopy. *syd-2* mutants show an increase in the total number of vesicles clustered in regions containing active zones (Table 1), yet synaptic transmission is impaired, suggesting that the active zones in *syd-2* are defective. The structural and functional defects of *syd-2* mutants are mild, which suggests that *syd-2* may function redundantly with other proteins. We propose that SYD-2 may act as a structural component of the active zones and/or as a cytoplasmic anchor to recruit other molecules to the active zones. This is

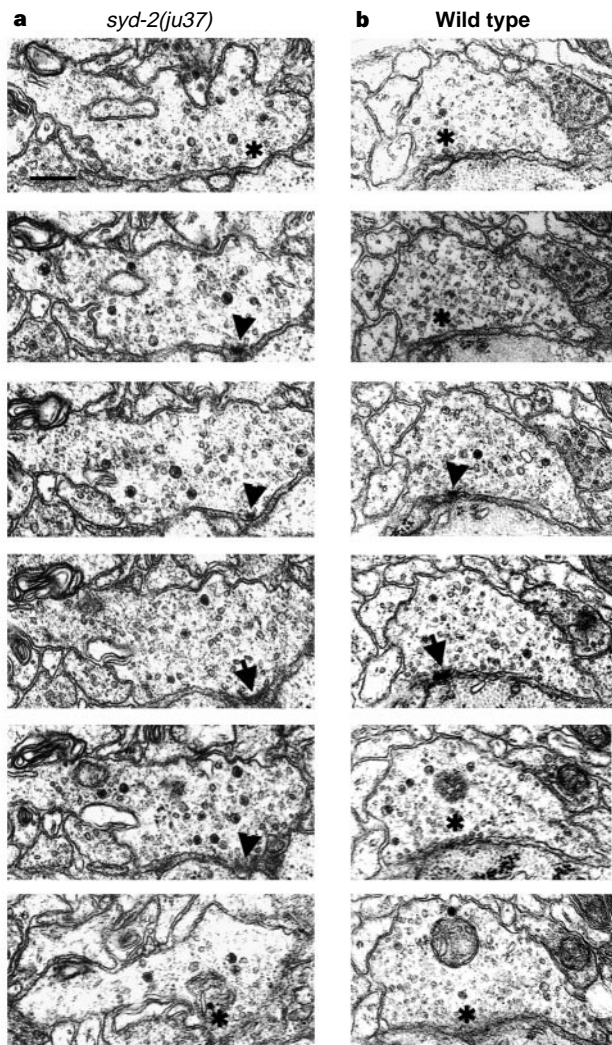


**Figure 4** Presynaptic active zones were lengthened in *syd-2(ju37)* animals. **a**, Serial electron micrographs (EMs) of a GABAergic NMJ made by the VD2 motor neuron in *syd-2(ju37)* animals. **b**, Serial EM sections of a GABAergic NMJ made by VD3 in wild-type animals. Arrows, prominent active zones; arrowheads, smaller active-zone structures; \* No active zones. Scale bar, 200 nm.

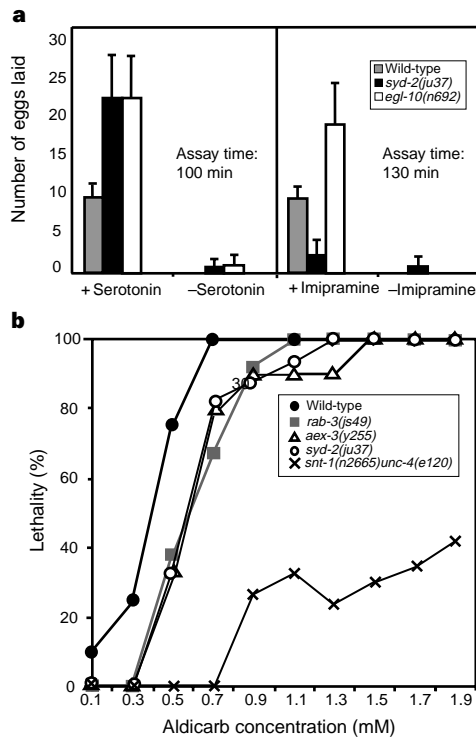


**Figure 5** Pharmacological responses of *syd-2(ju37)* animals. **a**, Serotonin but not imipramine stimulated *syd-2(ju37)* to lay eggs. *egl-10(n692)* (ref. 13) was used as a control. *syd-2(ju37)* and *egl-10(n692)* animals laid more eggs than did wild-type (N2) animals in both assays because they normally retained more eggs than did wild-type animals. Error bars, standard deviations ( $n = 12$ ). **b**, *syd-2(ju37)* was moderately resistant to aldicarb, comparable to *rab-3(js49)* and *aex-3(y255)*.

consistent with the observation that mammalian liprins recruit RPTPs to focal adhesions, and may thus regulate the disassembly of focal adhesions<sup>5</sup>. The roles of RPTPs in synapse formation have not been examined. In *Drosophila*, RPTPs are required for axon defasciculation<sup>24</sup>, a process that may also involve disassembly of protein complexes mediating cell–cell interactions at membranes. *syd-2* is the first liprin identified by genetics and will provide an *in vivo* system for studying the signalling pathway in which liprins, and possibly RPTPs, are involved at synaptic junctions. □

**Methods**

**C. elegans genetics.**

Worms were grown on NGM plates at 22.5 °C as described<sup>25</sup>. *syd-2(ju37)* was isolated in strain CZ323 *sem-4(n1378); juIs1* after ethyl methane sulphonate mutagenesis (M.Z. and Y.J., unpublished). *syd-2(ju37)* was mapped to linkage group X based on the diffuse SNB-1::GFP phenotype, and was further localized between *unc-115(e2225)* and *egl-15(n484)*, in the vicinity of *vab-3(e648)*. From *unc-115(e2225) egl-15(n484)/syd-2(ju37)* heterozygotes, two out of four *Unc* non-*Egl* and three out of four *Egl* non-*Unc* recombinants segregated *syd-2*. From *unc-115(e2225)vab-3(e648)/syd-2(ju37)* heterozygotes, all four *Unc* non-*Vab* and none of three *Vab* non-*Unc* animals segregated *syd-2*.

**syd-2 cloning.**

Four cosmids from the *vab-3* region were injected into *syd-2(ju37)* mutants, and cosmid F59F5 was found to contain *syd-2* rescuing activity. A 12.7-kilobase (kb) *Bgl*II fragment from F59F5, containing F59F5.6, was cloned into pBluescript SK (Stratagene) to generate the clone pCZ#2. All other *syd-2* clones in Fig. 2a were generated from pCZ#2 following standard protocols. pCZ#14 was constructed using the GFP vectors provided by A. Fire (personal communication).

Germline transformation was performed using pRF4 as a co-injection marker as described<sup>26</sup>. Plasmids and cosmids were injected at 50–100 ng μl<sup>-1</sup> and 20–30 ng μl<sup>-1</sup>, respectively. Integrated stable lines were established from transgenic animals by X-ray-induced mutagenesis.

**Mosaic analysis of syd-2.**

CZ1123 *syd-2(ju37)juIs1; juEx169[syd-2(+); SUR-5::GFP]* was generated by co-injecting *syd-2(ju37)juIs1* animals with pCZ#2, a plasmid containing the wild-type *syd-2* genomic DNA, and pTG96, a plasmid containing the *SUR-5::GFP* DNA that expresses GFP in all somatic nuclei<sup>11</sup>. Animals that lost the *juEx169[syd-2(+); SUR-5::GFP]* extrachromosomal array in P<sub>1</sub> lineage retained *SUR-5::GFP* expression in neurons and hypodermis, but not in gut cells and body wall and vulval muscles. Animals that lost the array in the AB lineage expressed *SUR-5::GFP* in the nuclei of muscle and gut cells, but not in neurons and hypodermis. Five P<sub>1</sub>-loss mosaic and six AB-loss mosaic animals were examined for *juIs1* expression pattern, locomotion and egg laying.

**SYD-2 antibody production and immunocytochemistry.**

A His<sub>6</sub>-SYD-2 fusion protein containing amino acids 206–704 (from the *yk100c11* complementary DNA clone) was expressed in bacteria using the pRSETB vector (Qiagen) following the manufacturer's protocol, and used to immunize rabbits (Animal Pharm). Antiserum was affinity purified using an Affi-gel 15 column coupled with purified His<sub>6</sub>-SYD-2 following the manufacturer's instructions (Bio-Rad). Worm protein extracts were made in 3% SDS, 10% glycerol and 3% β-mercaptoethanol. On western blots the affinity-purified SYD-2 antibodies detected a protein of relative molecular mass 130,000 (130K) which corresponds to the predicted size for full-length SYD-2 and was present only in wild-type worms. The anti-SYD-2 antibodies also detected a 96K protein that was present in both wild-type and *syd-2(ju37)* worms (Fig. 2c). We concluded that this 96K protein was not from the *syd-2* locus for the following reasons: the amount of this protein was unchanged in lysates of animals that overexpressed *syd-2*; the size of the protein was unchanged in lysates of animals carrying a rescuing GFP-tagged full-length SYD-2 transgene, whereas the 130K protein was shifted to the expected higher molecular weight; and no alternative RNA splice forms were detected from *syd-2* by RT-PCR.

Whole-mount immunofluorescent staining was performed as described<sup>27</sup>. Anti-SYD-2 antibodies were used at 0.03 μg μl<sup>-1</sup> on western blots and 6 μg μl<sup>-1</sup> on whole mounts. Monoclonal anti-GFP antibodies (from S. Mitani) were used at 0.2 μg μl<sup>-1</sup>. Cy5-conjugated goat anti-rabbit and FITC-conjugated goat anti-mouse IgG secondary antibodies (Cappel) were used at 0.375 μg μl<sup>-1</sup>.

**Drug tests.**

Aldicarb, serotonin and imipramine tests were performed as described<sup>13,20</sup>. All drug tests were scored blind and repeated at least three times.

**Electron microscopy.**

Wild-type (N2), CZ900 *syd-2(ju37)*, CZ458 *syd-2(ju37)juIs1* and CZ333 *juIs1* animals were fixed with glutaraldehyde and osmium tetroxide as described<sup>8</sup>. Fixed and embedded worms were first cut with glass knives at the posterior pharyngeal bulb. Starting from the anterior gonad, 200–400 serial thin sections of 60 nm thickness were collected for each sample. The ventral and/or dorsal nerve cords were photographed and examined. Chemical synapses were identified by the accumulation of synaptic vesicles around the

darkly stained membrane structures (active zones). GABAergic neuromuscular junctions (NMs) were identified as synapses to muscle arms made by DD/VD neurons, which lie on the outer surface of the ventral cord. Cholinergic NMs were identified as dyadic synapses to both DD or VD neurons and muscles<sup>8</sup>. Three N2 animals and two animals of each other genotype were examined. The data analysis was carried out by a double-blind test.

Received 24 March; accepted 19 July 1999.

1. Landis, D. M. D., Hall, A. K., Weinstein, L. A. & Reese, T. S. The organization of cytoplasm at the presynaptic active zone of a central nervous system synapse. *Neuron* **1**, 201–209 (1988).
2. Südhof, T. C. The synaptic vesicle cycle: a cascade of protein–protein interactions. *Nature* **375**, 645–653 (1995).
3. Nonet, M. L. Visualization of synaptic specializations in live *C. elegans* with synaptic vesicle protein-GFP fusions. *J. Neurosci. Methods* **89**, 33–40 (1999).
4. Hallam, S. & Jin, Y. *lin-14* regulates the timing of synaptic remodeling in *Caenorhabditis elegans*. *Nature* **395**, 78–80 (1998).
5. Serra-Pages, C. *et al.* The LAR transmembrane protein tyrosine phosphatase and a coiled-coil LAR-interacting protein co-localize at focal adhesions. *EMBO J.* **14**, 2827–2838 (1995).
6. Serra-Pages, C., Medley, Q. G., Tang, M., Hart, A. & Streuli, M. Liprins, a family of LAR transmembrane protein-tyrosine phosphatase-interacting proteins. *J. Biol. Chem.* **273**, 15611–15620 (1998).
7. Rand, J. B. & Nonet, M. Synaptic transmission. In *C. elegans II* (eds Riddle, D., Blumenthal, T., Meyer, B. & Priess, J. R.) 611–643 (Cold Spring Harbor Laboratory Press, New York, 1997).
8. Jin, Y., Jørgensen, E., Hartwig, E. & Horvitz, H. R. The *Caenorhabditis elegans* gene *unc-25* encodes glutamic acid decarboxylase and is required for synaptic transmission but not synaptic development. *J. Neurosci.* **19**, 539–548 (1999).
9. White, J. G., Southgate, E., Thomson, J. N. & Brenner, S. The structure of the nervous system of the nematode *Caenorhabditis elegans*. *Phil. Trans. R. Soc. Lond. B* **314**, 1–340 (1986).
10. Stapleton, D., Balan, I., Pawson, T. & Sicheri, E. The crystal structure of an Eph receptor SAM domain reveals a mechanism for modular dimerization. *Nature Struct. Biol.* **6**, 44–49 (1999).
11. Yochem, J., Gu, T. & Han, M. A new marker for mosaic analysis in *Caenorhabditis elegans* indicates a fusion between *hyp6* and *hyp7*, two major components of hypodermis. *Genetics* **149**, 1323–1334 (1998).
12. Hall, H. & Hedgecock, M. Kinesin-related gene *unc-104* is required for axonal transport of synaptic vesicles in *C. elegans*. *Cell* **65**, 837–847 (1991).
13. Trent, C., Tsung, N. & Horvitz, H. R. Egg-laying defective mutants of the nematode *C. elegans*. *Genetics* **104**, 619–647 (1983).
14. Burns, M. E. & Augustine, G. J. Synaptic structure and function: dynamic organization yields architectural precision. *Cell* **83**, 187–194 (1995).
15. Thomas, U. *et al.* Synaptic clustering of the cell adhesion molecule Fasciclin II by Discs-Large and its role in the regulation of presynaptic structure. *Neuron* **19**, 787–799 (1997).
16. Sone, M. *et al.* Still life, a protein in synaptic terminals of *Drosophila* homologous to GDP-GTP exchangers. *Science* **275**, 543–547 (1998).
17. Rosahl, T. W. *et al.* Essential functions of synapsins I and II in synaptic vesicle regulation. *Nature* **375**, 488–493 (1995).
18. Wang, Y., Okamoto, M., Schmitz, F., Hofmann, K. & Südhof, T. C. Rim is a putative RAB3 effector in regulating synaptic-vesicle fusion. *Nature* **388**, 593–598 (1997).
19. tom Dieck, S. *et al.* Bassoon, a novel zinc-finger CAG/Glutamine-repeat protein selectively localized at the active zone of presynaptic nerve termini. *J. Cell Biol.* **142**, 499–509 (1998).
20. Jørgensen, E. *et al.* Defective recycling of synaptic vesicles in synaptotagmin mutant of *Caenorhabditis elegans*. *Nature* **378**, 196–199 (1995).
21. Nonet, M. *et al.* *Caenorhabditis elegans rab-3* mutant synapses exhibit impaired function and are partially depleted of vesicles. *J. Neurosci.* **17**, 8061–8073 (1997).
22. Betz, W. J. & Henkel, A. W. Okadaic acid disrupts clusters of synaptic vesicles in frog motor nerve terminals. *J. Cell Biol.* **124**, 843–854 (1994).
23. Kraszewski, K. *et al.* Synaptic vesicle dynamics in living cultured hippocampal neurons visualized with CY3-conjugated antibodies directed against the luminal domain of synaptotagmin. *J. Neurosci.* **15**, 4328–4342 (1995).
24. Desai, C. J., Gindhart, J. G. Jr, Goldstein, L. S. & Zinn, K. Receptor tyrosine phosphatases are required for motor axon guidance in the *Drosophila* embryo. *Cell* **84**, 599–609 (1996).
25. Brenner, S. The genetics of *Caenorhabditis elegans*. *Genetics* **77**, 71–94 (1974).
26. Mello, C. C., Kramer, J. M., Stinchcomb, D. & Ambros, V. Efficient gene transfer in *C. elegans*: extrachromosomal maintenance and integration of transforming sequence. *EMBO J.* **10**, 3959–3970 (1991).
27. Finney, M. & Ruvkun, G. B. The *unc-86* gene product couples cell lineage and cell identity in *C. elegans*. *Cell* **63**, 895–905 (1990).
28. Hedgecock, E. M., Culotti, J. G. & Hall, D. H. The *unc-5*, *unc-6*, *unc-40* genes guide circumferential migrations of pioneer axons and mesodermal cells on the epidermis in *C. elegans*. *Neuron* **2**, 61–85 (1990).

**Acknowledgements**

We thank M. Nonet for SNB-1::GFP DNA and antibodies for SNT-1, SNB-1, syntaxin and RAB-3; Y. Kohara for the *yk100c11* clone; A. Fire for the GFP vectors; M. Han for the pTG96 plasmid; C. *elegans* genome consortium for the sequence and clone of cosmid F59F5; A. Chisholm, E. Jørgensen and M. Nonet for helpful discussion throughout this work; E. Hartwig for teaching us electron micrograph analysis; and R. Horvitz for his generosity. A. Chisholm, J. Kaplan, G. Garriga, L. Hinck, A. Zahler, R. Baran, Y. Ho and members of the Chisholm and Jin laboratories made comments on this paper. Some strains used in this work were obtained from the *Caenorhabditis elegans* Genetics Center, which is funded by NIH Center for research resources. M.Z. is supported by a Human Frontier Science Program Long Term Postdoctoral Fellowship. Y.J. is a Alfred P. Sloan research fellow. This work was supported by US PHS research grant NS35546 to Y.J. The GenBank accession numbers for *syd-2* genomic DNA and cDNA are Z50794 and AF170122, respectively.

Correspondence and requests for materials should be addressed to Y.J. (e-mail: jin@biology.ucsc.edu).